a *control^{RNAi}; indy-GFP*

DNA membrane GFP F-actin

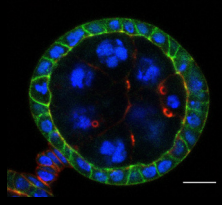

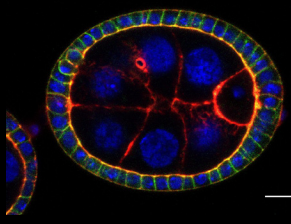

stage	4	5
number of cells	184 ± 34 s.d.	413 ± 50 s.d.
aspect ratio	1.16 ± 0.07 s.d.	1.34 ± 0.06 s.d.
volume (μm^3)	60,838 ± 1,1192 s.d.	107,630 ± 2,1727 s.d.
nurse cell nuclear diameter (μm)	N/A (polytene)	12.95 ± 1.22 s.d.

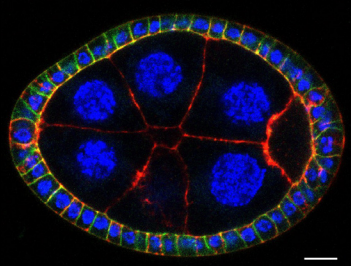

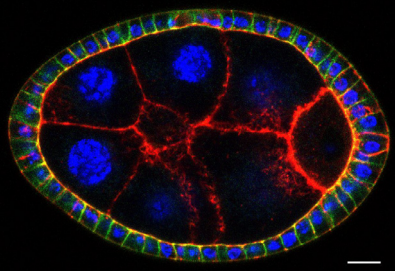

stage	6A	6B
number of cells	550 ± 44 s.d.	751 ± 66 s.d.
aspect ratio	1.42 ± 0.12 s.d.	1.54 ± 0.12 s.d.
volume (μm^3)	131,636 ± 32,104 s.d.	219,000 ± 8,0991 s.d.
nurse cell nuclear diameter (μm)	14.28 ± 1.95 s.d.	15.59 ± 2.61 s.d.

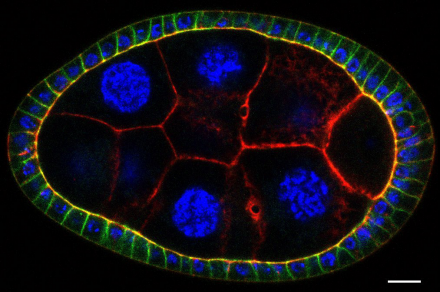

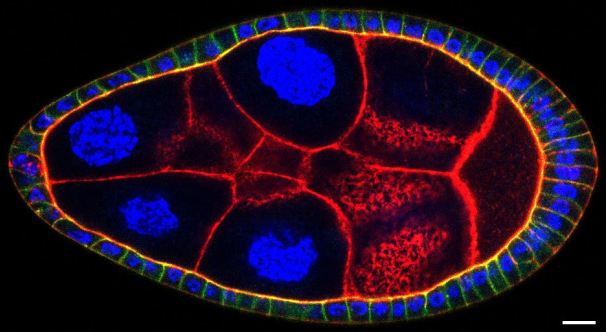

stage	7	8
number of cells	887 ± 33 s.d.	862 ± 28 s.d.
aspect ratio	1.82 ± 0.09 s.d.	1.91 ± 0.07 s.d.
volume (μm^3)	334062 ± 49880 s.d.	552705 ± 91295 s.d.
nurse cell nuclear diameter (μm)	19.86 ± 3.05 s.d.	23.64 ± 1.66 s.d.

10 μm

b

Stage	Duration by Lin&Spradling (h)	Duration by David&Merle (h)	Approx. range of follicle cell number	Approx. range of nurse cell nucleus diameter (μm)
4	6	9.16	125-300	N/A (polytene)
5	5	2.61	300-500	11-14
6A	3	8.45	500-650	14-15
6B			650-850	15-17
7	6	8.69	850+	17-21
8	6	5.21	850+	21+

Supplementary Fig. 1

Supplementary Figure 1| a, Morphometric data for follicles staged by cell number, which generally correlate with classic morphological criteria. Values shown are average ± standard deviation (s.d.) **b**, Table showing durations of stages according to Lin and Spradling (1993) deduced from single ovariole transplants into *ovoD1* female hosts, or David and Merle (1968) deduced from representation of follicle stages in WT hosts; Approximate range of follicle cell number and nurse cell nucleus diameter for suggested staging.

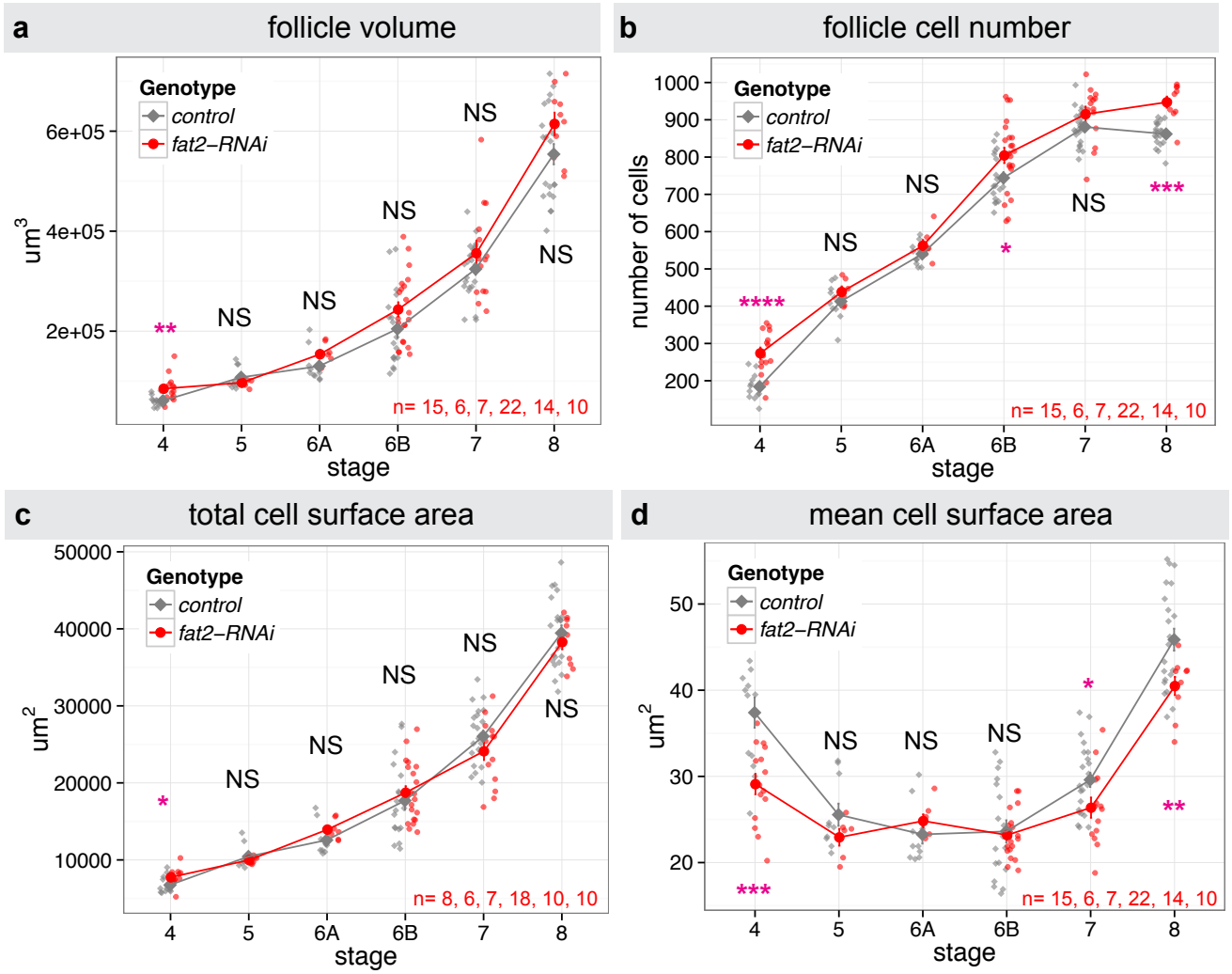

Supplementary Fig. 2

Supplementary Figure 2| a-d, Further morphometric data of follicle volume(**a**), cell number(**b**), total cell surface area(**c**), and mean cell surface area(**d**) comparing control to *fat2*-depleted follicles. **e,** Example from ImSAnE cylinder projection showing mitotic spindle (yellow arrowhead) in control st.6 follicle rotating from initial latitudinal orientation to final AP-oriented cell division (see also **Video 3**). n, Sample size. NS, not significant, *P<0.5, **P<0.01, ***P<0.001. Error bars, s.e.m.

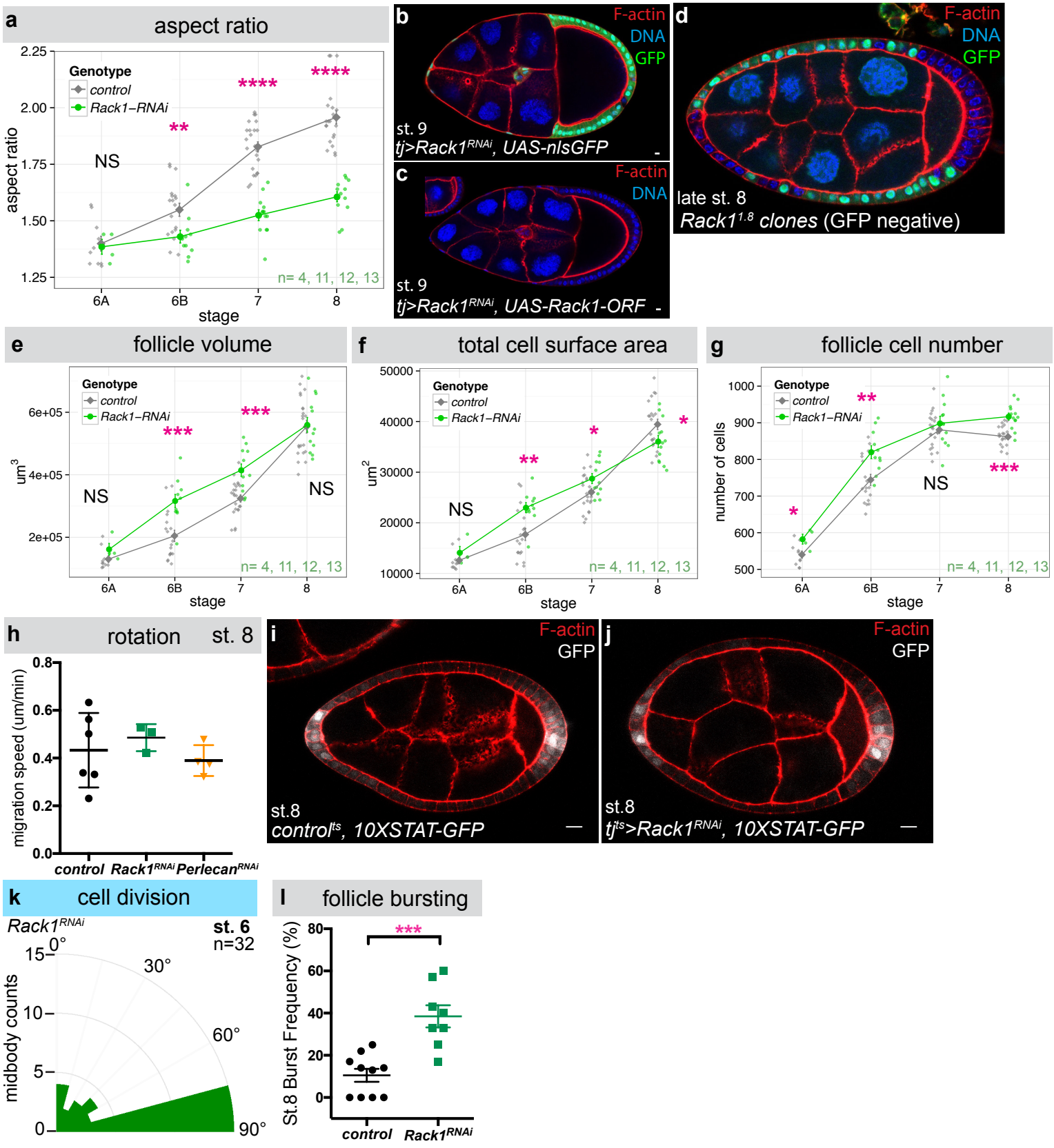

Supplementary Fig. 3

Supplementary Figure 3| a, Elongation of *Rack1*-depleted follicles diverges from control at st. 6B. **b-c,** *Rack1*-depleted round follicle phenotype is rescued by overexpression of the *Rack1*-ORF. **d**, Mitotic clones of a *Rack1* null allele (marked by absence of GFP) perturb elongation. **e-g**, Further morphometric data of follicle volume(**e**), total cell surface area(**f**), and follicle cell number(**g**) comparing control to *Rack1*-depleted follicles. **h**, Both *Rack1 and Perlecan*-depleted follicles undergo rotation (see also **Video 4**). **i-j**, *Rack1*-depleted follicles show normal STAT activity gradients(gray) at poles, and **k,** undergo oriented cell divisions at st. 6 (n=32) similar to control. **l,** Bursting frequency under osmotic stress is increased compared to control follicles. n, Sample size. NS, not significant, *P<0.5, **P<0.01, ***P<0.001, ****P<0.0001.

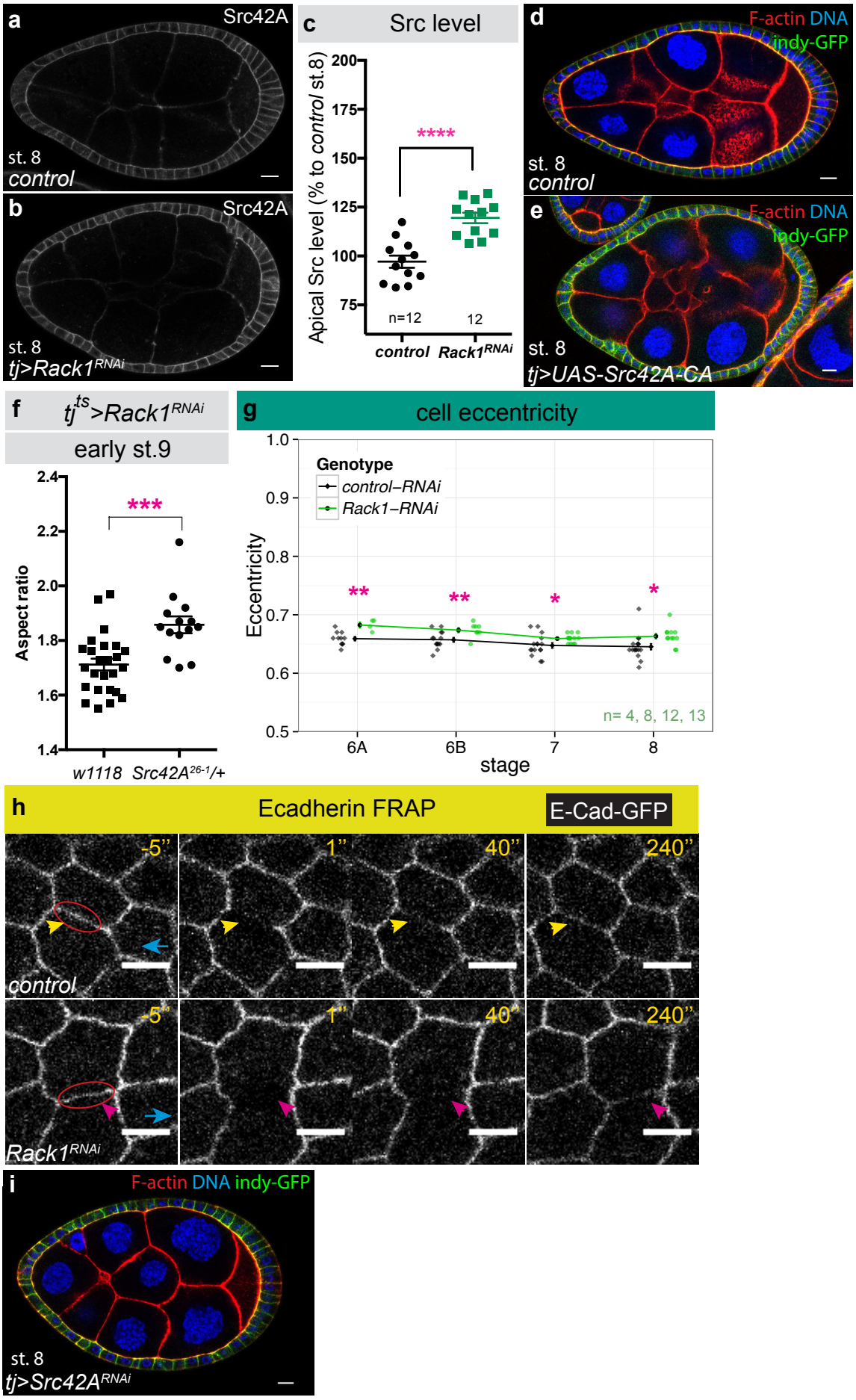

Supplementary Fig. 4

Supplementary Figure 4| a-c, Levels of total Src42A protein (gray) are increased in *Rack1*-depleted follicles. **d-e**, Hyperactivation of Src42A, like its depletion, impairs follicle elongation. **f**, Heterozygosity for *Src42A* partially suppresses elongation defects of *Rack1*-depleted follicles. **g**, Cell eccentricity is slightly increased when Rack1 is depleted. **h**, FRAP recovery is not through lateral diffusion. Yellow and magenta arrows mark photobleached junctions; blue arrows indicate direction of follicle rotation. **i,** *Src42A*-depleted follicle has impaired follicle elongation. n, Sample size. Scale bars, 100 μm. *P<0.5, **P<0.01, ***P<0.001, and ****P<0.0001.